Impact of Acquisition Geometry, Image Processing, and Patient Size on Lesion Detection in Whole-Body ^{18}F-FDG PET

Georges El Fakhri[1], Paula A. Santos[2,1], Ramsey D. Badawi[3], Clay H. Holdsworth[4], Annick D. Van Den Abbeele[5], and Marie Foley Kijewski[1]

[1]*Division of Nuclear Medicine, Department of Radiology, Harvard Medical School and Brigham and Women's Hospital, Boston, Massachusetts;* [2]*Biophysics and Biomedical Engineering Institute, Faculty of Sciences, University of Lisbon, Lisbon, Portugal;* [3]*Department of Radiology, University of California Davis Medical Center, Sacramento, California;* [4]*Massachusetts College of Pharmacy and Health Sciences, Boston, Massachusetts; and* [5]*Department of Radiology, Dana Farber Cancer Institute, Boston, Massachusetts*

The aim of this work was to develop a rigorous evaluation methodology to assess performance of different acquisition and processing methods for variable patient sizes in the context of lesion detection in whole-body ^{18}F-FDG PET. **Methods:** Fifty-nine bed positions were acquired in 32 patients in 2-dimensional (2D) and 3-dimensional (3D) modes 1–4 h after ^{18}F-FDG injection (740 MBq) using a BGO PET scanner. Three spheres (1.0-, 1.3-, and 1.6-cm diameter) containing ^{68}Ge were also imaged separately in air, at locations corresponding to possible lesion sites in 2D and 3D (590 targets per condition). Each bed position was acquired for 7 min in 2D and 6 min in 3D and corrected for randoms using delayed window randoms subtraction (DWS) or randoms variance reduction (RVR). Sphere sinograms were attenuated using the 2D or 3D attenuation map derived from the transmission scan of the patient, after scaling 2D and 3D sinograms with identical factors to ensure marginal detectability. Resulting 2D sinograms were reconstructed with filtered backprojection (FBP) and ordered-subsets expectation maximization (OSEM) without any scatter or attenuation correction (FBP-NATS and OSEM-NATS) or corrected for scatter and attenuation and reconstructed using FBP (FBP-ATT) or attenuation-weighted OSEM (AWOSEM). 3D sinograms were processed identically after Fourier rebinning. Next, reconstructed volumes were compared on the basis of performance of a 3-channel Hotelling observer (CHO-SNR [SNR is signal-to-noise ratio]) in detecting the presence of a sphere of unknown size on an anatomic background while modeling observer noise. The noise equivalent count (NEC) rate was computed in 2D and 3D for 3 different phantoms sizes (40, 60, and 95 kg) and compared with lesion detection SNR. **Results:** 3D imaging yielded better lesion detectability than 2D ($P < 0.025$, 2-tailed paired t test) in patients of normal size (body mass index [BMI] ≤ 31). However, 2D imaging yielded better lesion detectability than 3D in large patients (BMI > 31), as 3D performance deteriorated in large patients ($P < 0.05$). 2D and 3D yielded similar results for different lesion sizes. CHO-SNR were 40% greater for AWOSEM, FBP-ATT, and FBPNAT than for OSEM ($P < 0.05$), and AWOSEM yielded significantly better lesion detectability than did FBP. In all patients, RVR yielded a systematic improvement in CHO-SNR over DWS in both 2D and 3D. $\sqrt{\text{NEC}}$ was characterized by a behavior similar to that of SNR_{CHO} for the 3 different phantom sizes considered in this study.

Key Words: whole-body ^{18}F-FDG PET; 2D/3D acquisition; lesion detection; numeric observer

J Nucl Med 2007; 48:1951–1960
DOI: 10.2967/jnumed.108.007369

Three-dimensional (3D) "septumless" whole-body (WB) ^{18}F-FDG PET yields increased sensitivity to true coincidences at the expense of increased sensitivity to scattered and random coincidences. Several groups have assessed the relative merits of 3D and 2-dimensional (2D) WB-PET for BGO-based PET scanners using numeric simulations, phantom studies, or patient studies, applying various metrics. Raylman et al. (*1*), in a single-observer subjective visibility phantom study, reported equal performance for 2D and 3D PET, whereas Moore et al. (*2*) reported higher nonprewhitening signal-to-noise ratio for 3D than for 2D in a study using an anthropomorphic torso phantom. On the other hand, Farquhar et al. (*3*) reported significantly better performance in detecting simulated lesions on normal patient background images with 2D than with 3D WB ^{18}F-FDG PET, with a 3D performance close to the line of chance. Lartizien et al. (*4,5*) reported, on the basis of human and numeric observer detectability studies using numeric simulations of the MCAT torso phantom (Mathematical Cardiac Torso phantom), better performance with 2D PET and a 740-MBq injection of ^{18}F-FDG than with 3D PET with a 444-MBq injection. They found, however, that detectability with 3D PET was greater than or similar to that of 2D PET if a 444-MBq injection was simulated for both modes. Visvikis et al. (*6*) reported that human observers, asked to subjectively assess WB scans, rated

Received Jul. 29, 2006; revision accepted Aug. 24, 2007.
For correspondence or reprints contact: Georges El Fakhri, PhD, Department of Radiology, Brigham and Women's Hospital, Harvard Medical School, Boston, MA 02115.
E-mail: elfakhri@bwh.harvard.edu

Representative Results:

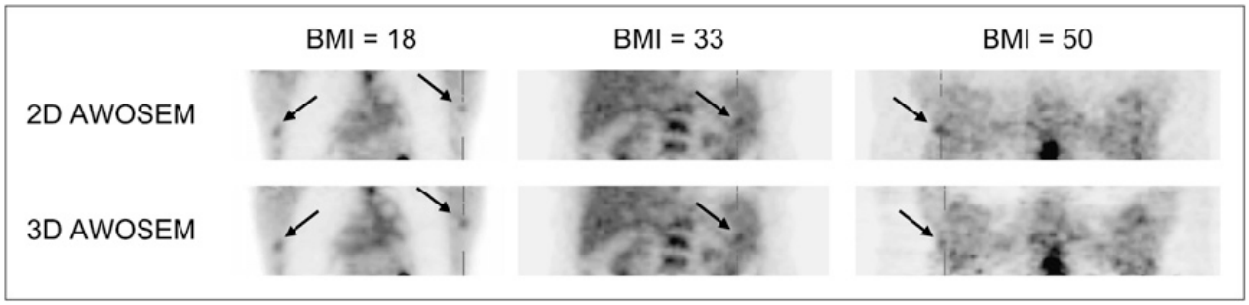

FIGURE 5. Lesion-present (arrow) coronal slices through normal-weight (BMI = 18, 2 lesions shown), obese (BMI = 33, 1 lesion shown), and extremely obese (BMI = 50, 1 lesion shown) patient studies in 2D and 3D modes reconstructed using the clinical protocol (AWOSEM).

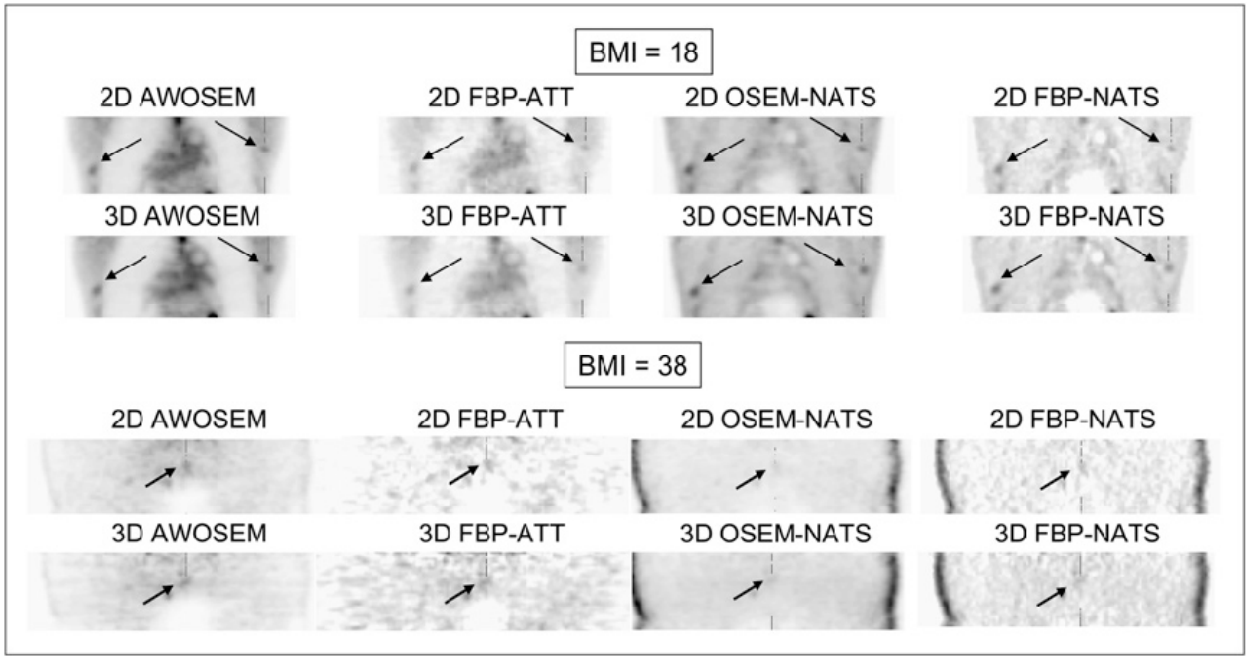

FIGURE 8. Coronal slices through normal-weight patient (BMI = 18) and obese patient (BMI = 38) in 2D and 3D corresponding to the following image processing protocols: FBP with (FBPATT) and without (FBP-NATS) attenuation and scatter corrections, OSEM without attenuation and scatter corrections (OSEM-NATS) and attenuation-weighted OSEM (AWOSEM). Arrows point to lesions added in mediastinum. Randoms were compensated for using the RVR technique.